

LUNAR-VISE: AN INVESTIGATION OF THE MOON'S NON-MARE SILICIC VOLCANISM. K. Donaldson Hanna¹, J. Benavente², K. Bennett³, B. Denevi⁴, A. Dove¹, J. Hagerty³, C. Hardgrove⁵, P. Hayne⁶, A. LaMee¹, M. Landis⁶, D. Osterman⁷, T. Prettyman⁸, K. A. Shirley⁹, M. Siegler⁸, J. Sunshine¹⁰, J-P. Williams¹¹, S. Valencia¹⁰, Ball Aerospace team⁷, and Arizona State University team⁵, ¹University of Central Florida (Kerri.DonaldsonHanna@ucf.edu), ²PMSS, ³US Geological Survey, ⁴Johns Hopkins Applied Physics Laboratory, ⁵Arizona State University, ⁶University of Colorado Boulder, ⁷Ball Aerospace, ⁸Planetary Science Institute, ⁹University of Oxford, ¹⁰University of Maryland, and ¹¹University of California Los Angeles.

Background: The Gruithuisen domes (36°N, 40°W) were first identified as volcanic structures distinct from their surrounding mare flows based on their distinct morphology and unusually red-sloped UV-visible spectrum [e.g., 1–3]. Morphologic analyses of the steep-sided domes suggested they are composed of highly viscous magmas similar to terrestrial extrusive volcanic features, which are consistent with higher silica contents (> 52 wt% SiO₂) found in rhyolites, dacites and basaltic andesites [e.g., 4]. Further observations by Lunar Prospector (LP), Diviner Lunar Radiometer (Diviner), and the Lunar Reconnaissance Orbiter Camera (LROC) have shown that the domes are enriched in Th (~17 to 40 ppm) and SiO₂, and low in FeO [e.g., 5–7]. However, the exact composition of the rock making up the domes has remained elusive. In particular, Diviner's compositional bands were not optimized for constraining the composition of highly silicic materials [6,8], making it challenging to constrain how such rocks could form on a single plate planetary body like the Moon.

Mission Objectives: The Lunar Vulkan Imaging and Spectroscopy Explorer (Lunar-VISE) was selected as part of Payloads and Research Investigations on the Surface of the Moon (PRISM) 2 for Task Order (TO) CP-21. Lunar-VISE will land on the Gruithuisen Gamma dome and will use its combined lander and rover payload to determine the composition and physical properties of the rocks and regolith comprising the domes, placing critical constraints on their formation mechanism.

Our investigation has one high-level science goal and one exploration goal. Our overarching science goal is to understand how late-stage lunar silicic volcanism works, as typified by the Gruithuisen domes. This goal is accomplished through two science objectives that place critical constraints on the two main hypotheses for the formation of non-mare silicic volcanic constructs by (1) mapping spatial variations in composition along multiple traverses across the landing site, and correlating the measured variations to rock and regolith properties, surface features, and dome morphology. Lunar-VISE will also (2) relate those local-scale measurements to orbital remote sensing observations from previous and current spacecraft. Our primary exploration goal is to understand the geotechnical properties of the lunar regolith on the domes at the lander/rover scale. This exploration goal is accomplished by mapping local variations in regolith properties of the region surrounding the landing site and along the rover's traverse.

Lunar-VISE Instrument Suite: To achieve our goals and objectives, Lunar-VISE includes a complementary suite of heritage instruments on a rover and lander (see **Fig. 1**). The rover payload includes two separate units, the Lunar-VISE Visible/Infrared Multiband Suite (LV-VIMS) and the Gamma Ray and Neutron Spectrometer (LV-GRNS).

LV-VIMS is an instrument suite combining two multispectral imaging instruments in a single enclosure: the VNIR Imaging Camera (LV-VIC) and the Compact Infrared Imaging System (LV-CIRiS). From their location on top of the rover, these multispectral cameras image the landscape in panoramic scans up to 180°, LV-VIC and LV-CIRiS are co-boresighted and, rotate together on a common stage. LV-VIC (**Fig. 1**) draws heritage from Ball Aerospace's GeoSpace Camera



(BGSC), a production-ready visible camera originally designed for NASA's Orion program. LV-CIRiS (**Fig. 1**) draws heritage from Ball's CIRiS instrument, now operating in low Earth orbit on a CubeSat spacecraft and L-CIRiS built for delivery to the lunar south pole in 2027. LV-VIC spectral channels were chosen to be at similar wavelengths to those on the Clementine, LROC Wide Angle Camera, and Kaguya Multiband Imager. The three compositional channels of LV-CIRiS were specifically chosen to estimate the SiO₂ content of highly silicic regions and are at similar wavelengths as on Diviner, L-CIRiS, and Lunar Trailblazer. Further details on the field of view and spectral channels of LV-VIC and LV-CIRiS are given in **Table 1**.

The LV-GRNS is located on the front of the rover where it acquires measurements of gamma rays and neutrons emitted from the lunar surface, both spanning the energy range needed to quantify critical elements including Si, Fe, and Th. LV-GRNS is a rebuild, with minor modifications, of the Miniature Neutron Spectrometer (Mini-NS, **Fig. 1**) launched on LunaH-Map in November 2022. The GRNS incorporates two sensor heads, each with a cylindrical 7.6 cm (3") diameter CLYC scintillator crystal coupled to its own photomultiplier tube (PMT).

The lander suite includes two additional cameras for characterizing the landing site and rover traverse: the nadir-facing Lunar-VISE descent camera (LV-DC) for surface imaging during landing, and the side-mounted Lunar-VISE context camera (LV-CC) for a > 270° panorama around the landing site and rover traverse. Both cameras are build-to-print copies of the LV-VIC (**Fig. 1**) but without the multispectral capabilities.

Table 1. LV-VIMS field of view (FOV) and filter parameters.

| | LV-VIC | LV-CIRiS |
|-----------------------------------|-------------------------|------------------|
| Field of Regard (Elv × Az) | 19.1° × 180° | 17.5° × 180° |
| Fore/Background Range | 3.2m to infinity | 3.6m to infinity |
| Spectral Bands | All bandwidths 20 nm | |
| 1 | 360 nm | 7.20 – 7.40 μm |
| 2 | 415 nm | 7.35 – 7.65 μm |
| 3 | 566 nm | 7.65 – 7.95 μm |
| 4 | 675 nm | 8.0 – 14.0 μm |
| 5 | 750 nm | |
| 6 | 900 nm | |
| 7 | 950 nm | |

Landing Site and Concept of Operations: We have identified several suitable landing sites on

relatively flat slopes (< 5°, **Fig. 2**) on the Gamma and Delta domes. For the Lunar-VISE science and exploration goals to be met, the candidate landing sites need to have access to boulders, possible exposures of original bedrock in impact craters, and should ideally be located near the edge of the dome to enable multispectral imaging of the surrounding maria. In particular, the region on the Gamma dome highlighted in the red box is an example that meets these criteria. The baseline mission includes observations that include: (1) both the area immediately around the landing site, which has been disturbed during landing, and undisturbed regolith outside the scoured landing region using the LV-CC and LV-DC cameras on the lander and the LV-VIMS and the LV-GRNS on the rover, (2) dome regolith and boulders by LV-VIMS and LV-GRNS, and (3) the rover traversing through the regolith by the LV-CC.

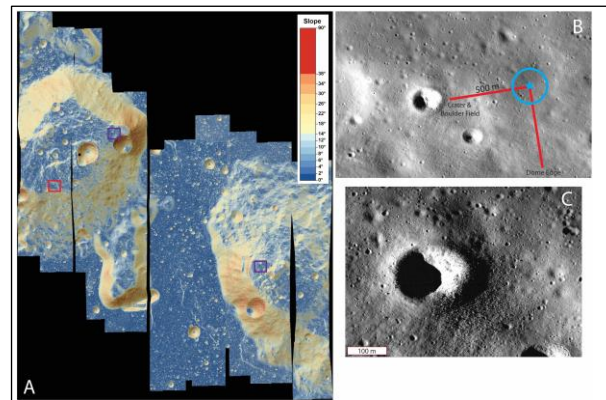


Figure 2. (A) LROC NAC STM slope map highlighting 3 possible landing sites on the Gamma and Delta domes. (B) WAC image showing a possible landing site on the Gamma dome marked in the red box in A. The two red lines indicate the maximum 500 m rover traverse length, showing the area that could be explored, and the blue circle highlighting a 100 m landing ellipse. (C) NAC image showing an abundant boulder field around the small crater shown in B.

Acknowledgments: Lunar-VISE is funded through NASA's PRISM2 cooperative agreement number 80NSSC22M0303. Thanks to our Mission Manager M. Selby, Program Scientist R. Watkins, Project Scientist J. Karcz, CLPS Integration Manager J. Schonfeld, and NASA HQ and PMPO teams.

References: [1] Head J. W. and McCord T. B. (1978) *Science*, 199, 1433-1436. [2] Bruno B. C. et al. (1991) *LPSC XXI*, 405-415. [3] Chevrel S. D. et al. (1999) *JGR*, 104, 16515-16529. [4] Wilson L. and Head J. W. (2003) *JGR Planets*, 108(E2), 5012. [5] Hagerty J. J. et al. (2006) *JGR*, 111, doi:10.1029/2005JE002592. [6] Glotch T. D. et al. (2010) *Science*, 329, 1510-1513. [7] Clegg-Watkins R. N. (2017) *Icarus*, 285, 169-184. [8] Greenhagen B. T. et al. (2010) *Science*, 329, 1507-1509.